

ORIGINAL ARTICLE

Silvalactam, a 24-membered macrolactam antibiotic produced by *Streptomyces* sp. Tü 6392*

Dirk Schulz^{1,2}, Jonny Nachtigall³, Ulf Geisen⁴, Holger Kalthoff⁴, Johannes F Imhoff², Hans-Peter Fiedler¹ and Roderich D Süssmuth³

Streptomyces were isolated out of a soil sample taken from the rhizosphere of a spruce stand and screened by HPLC–diode array analysis for the production of secondary metabolites. This led to the detection of silvalactam, a novel 24-membered macrolactam antibiotic in extracts of *Streptomyces* strain Tü 6392. The structure was determined by MS and NMR spectroscopy experiments. Silvalactam shows a potent antiproliferative activity against various cancerous and non-cancerous cell lines.

The Journal of Antibiotics (2012) 65, 369–372; doi:10.1038/ja.2012.33; published online 9 May 2012

Keywords: antitumor agent; 24-membered macrolactam antibiotic; *Streptomyces*

INTRODUCTION

Streptomyces from soils are still a rich source of novel secondary metabolites with diverse biological activities.^{2,3} We isolated several actinomycetes strains from the rhizosphere of a spruce stand and investigated them for production of novel secondary metabolites. The rhizosphere is a habitat with a high abundance of microbes—bacteria and fungi—promoted by plant exudates released through the roots. In this environment, microbes are exposed to a permanent competition, where the production of specific antibiotics may be a decisive advantage to survive within the microbial community.

The isolated *Streptomyces* strains were grown in shake flasks in various complex media,⁴ and extracts were analyzed by HPLC–diode array monitoring and evaluated by means of an in-house HPLC–UV–Vis database to detect novel secondary metabolites.⁵ By this technique, strain Tü 6392 was found to produce silvalactam (**1**), a new member of the family of macrolactam antibiotics, which is mainly produced by streptomyces and which is distinguished by various biological activities.⁶ The structure of **1** is shown in Figure 1.

Recently, we published the 23-membered macrolactam antibiotic piceamycin showing cytotoxic and antibacterial activity, which is also produced by a soil-associated *Streptomyces* strain isolated from the rhizosphere.⁷

RESULTS

Taxonomy of the producing strain

Strain Tü 6392 was isolated from a soil sample taken from the upper rhizosphere of a Norway spruce stand in the Rammert Forest near Tübingen (Germany). The morphological and chemical properties of strain Tü 6392 designated the strain as a member of the genus

Streptomyces.^{8,9} Whole-cell hydrolysates of strain Tü 6392 showed the presence of LL-diaminopimelic acid in the peptidoglycan. The predominant isoprenologs found were hexa- and octahydrogenated menaquinones with nine isoprene units. Partial sequencing of the 16S rRNA gene confirmed its taxonomic classification to the genus *Streptomyces*.

Fermentation and isolation

Strain Tü 6392 was cultivated in 500-ml shake flasks in SGG medium. Extracts of the culture filtrates and mycelium extracts were analysed by HPLC–diode array and gave a dominant peak at 9.4 min in the chromatogram with a characteristic UV–visible spectrum that differed from those of 960 reference compounds stored in our in-house HPLC–UV–Vis database.⁵

Scale-up of the cultivation was performed in a 10-l stirred tank fermentor yielding an amount of 128 mg l⁻¹ of compound **1** at a fermentation time of 144 h. For isolation of **1**, a 5-l aliquot of the culture filtrate was extracted with EtOAc and purified by chromatography on a diol-modified silica gel column followed by preparative reversed-phase HPLC. About 24 mg of pure **1** was obtained as a pale yellowish powder.

Structure determination

The molecular mass of **1** was determined by high-resolution ESI–TOF (time-of-flight) MS, which gave the mass of 637.4194 suggesting a molecular formula of C₃₈H₅₆N₂O₆ (theoretical: 637.4211, $\Delta m = 2.67$ p.p.m.). The physicochemical properties of **1** are described in Table 1.

The ¹H-NMR spectrum of **1** showed 15 signals in the olefinic region, 3 signals between 4 and 5 p.p.m. and 17 signals in the aliphatic

¹Mikrobiologisches Institut, Universität Tübingen, Tübingen, Germany; ²Kieler Wirkstoff-Zentrum am Leibniz-Institut für Meereswissenschaften, Kiel, Germany; ³Institut für Chemie, Technische Universität Berlin, Berlin, Germany and ⁴Institut für experimentelle Tumorforschung, Sektion für Molekulare Onkologie, Universität Kiel, Kiel, Germany
Correspondence: Professor RD Süssmuth, Institut für Chemie, Technische Universität Berlin, Straße des 17. Juni 124, Berlin 10623, Germany.
E-mail: suessmuth@tu-berlin.de

*Art. No. 63 in 'Biosynthetic Capacities of Actinomycetes'. Art. No. 62: see Helaly *et al.*¹

Received 6 December 2011; revised 26 March 2012; accepted 28 March 2012; published online 9 May 2012

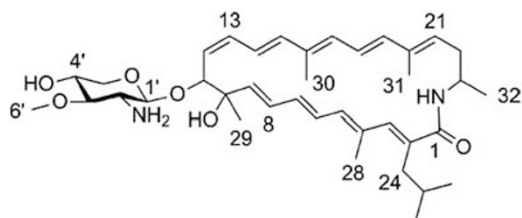


Figure 1 Structure of 1.

Table 1 Physicochemical properties of silvalactam (1)

Silvalactam (1)	
Appearance	Pale yellowish powder
MW	636
HR-ESI-MS (m/z)	
Measured (M + H) ⁺	637.4194
Calculated (M + H) ⁺	637.4211
Molecular formula	C ₃₈ H ₅₆ N ₂ O ₆
UV λ _{max} (MeOH) nm (ε)	309 (sh, 17310), 319 (19950), 359 (sh, 3960)
Optical rotation [α] _D ²⁰	−67° (c 0.075, MeOH)

region (Table 2). Integration of the signals revealed a total of 52 protons, with seven signals at δ_{H} 3.59, δ_{H} 2.03, δ_{H} 1.76, δ_{H} 1.70, δ_{H} 1.21, δ_{H} 1.14, δ_{H} 0.85 and δ_{H} 0.83 corresponding to methyl groups and one signal at δ_{H} 2.50 corresponding to a methylene group. The ¹³C-NMR, DEPT and the HSQC spectrum showed two additional methylene groups at δ_{C} 65.6 and δ_{C} 32.3, showing a total of eight methyl, three methylene, 21 methine and six quaternary carbon groups. The signal at δ_{H} 5.55 did not show a correlation in the HSQC spectra, suggesting the amide-NH origin of the signal. Further inspection of the 2D NMR data by means of COSY, HSQC and HMBC spectra allowed assignment of the structure of **1** (Figure 1) as follows. The ¹H-¹H-COSY spectrum revealed six spin systems for **1** (H-5-H-6-H-7-H-8-H-9, H-11-H-12-H-13-H-14-H-15, H-17-H-18-H-19, H-21-H-22-H-23-H-32-N-1, H-24-H-25-H-26-H-27 and between H-1'-H-2'-H-3'-H-4' and H-5') (Figure 2). The isolated spin system from H-5 to H-9 could be connected to the spin system from H-11 to H-15 through C-10 by the observation of the HMBC correlations from the methyl group H-29 to C-9, C-10 and C-11. The isolated spin system from H-11 to H-15 could be connected to the spin system from H-17 to H-19 through C-16 by the observation of the HMBC correlations from the methyl group H-30 to C-15, C-16 and C-17, and the spin system H-21 to N-1 could be joined together through C-20 by the observation of the HMBC correlation from the methyl group H-31 to C-19, C-20 and C-21 (Figure 2). Together with the HMBC correlation from H-28 to C-3, C-4 and C-5 and from H-24 to C-1, C-2 and C-3 the polyketide ring could be closed. Through the HMBC correlation from H-24 to C-1, C-2 and C-3 the spin system from H-24 to H-27 could be joined to give the carbon aglycon backbone. A weak HMBC correlation could be seen from the amide moiety 1-NH to C-1, establishing the ring closure across the lactam moiety. The nature of the double bonds of the aglycon of **1** was elucidated by means of seltOCOSY and NOESY spectra as follows. The coupling constants of $J_{6,7} = 15.6$ Hz, $J_{8,9} = 15.0$ Hz, $J_{12,13} = 11.2$ Hz, $J_{14,15} = 15.6$ Hz, $J_{18,19} = 14.9$ Hz revealed 6E, 8E, 12Z, 14E and 18E, respectively. NOEs observed between H-3-H-5, H-15-H-17 and H-19-H-21 revealed 2E, 4E, 16E and 20E, respectively. The NOESY correlation between H-1' and C-11 gave further evidence for the

Table 2 ¹H and ¹³C NMR data for silvalactam (1) in DCM-d₂ at 273 K

Position	Silvalactam (1)	
	δ_{C} , multiplicity	δ_{H} (J in Hz)
1	171.6, C	
2	137.1, C	
3	135.1, CH	6.15, s
4	134.2, C	
5	137.2, CH	5.93, d (11.3)
6	127.0, CH	6.42, dd (11.3, 15.6)
7	135.9, CH	6.03, dd (11.3, 15.6)
8	127.7, CH	6.28, dd (11.3, 15.0)
9	141.7, CH	5.82, d (15.0)
10	77.8, C	
11	88.8, CH	4.07, d (5.9)
12	125.7, CH	5.61, dd (5.9, 11.2)
13	133.4, CH	6.29, t (11.2)
14	128.9, CH	6.95, dd (11.2, 15.6)
15	137.0, CH	6.24, d (15.6)
16	136.5, C	
17	131.0, CH	6.24, d (11.2)
18	124.3, CH	6.53, dd (11.2, 14.9)
19	137.1, CH	6.40, d (14.9)
20	139.2, C	
21	126.7, CH	5.72, dd (4.4, 11.1)
22	32.3, CH ₂	1.98, m
		3.04, m
23	44.6, CH	4.11, m
24	36.0, CH ₂	2.50, d (6.9)
25	29.3, CH	1.60, tq (6.4, 6.7, 6.9)
26	22.4, CH ₃	0.85, d (6.4)
27	22.2, CH ₃	0.83, d (6.7)
28	15.9, CH ₃	2.03, s
29	24.8, CH ₃	1.14, s
30	12.9, CH ₃	1.76, s
31	12.5, CH ₃	1.70, s
32	19.1, CH ₃	1.21, d (6.8)
1-NH		5.55, d (7.7)
1'	106.7, CH	4.41, d (7.2)
2'	55.3, CH	2.76, dd (7.2, 7.6)
3'	85.1, CH	3.01, dd (7.6, 8.1)
4'	69.5, CH	3.72, m
5'	65.6, CH ₂	3.23, dd (11.1, 11.4)
		3.92, dd (4.7, 11.4)
6'	59.9, CH ₃	3.59, s

connection of the pentopyranose aminosugar moiety to C-11. The relative stereochemistry of the sugar moiety was deduced by the large coupling constants of $J_{1',2'_{\text{ax}}} = 7.2$ Hz, $J_{2',3'_{\text{ax}}} = 7.6$ Hz, $J_{3',4'_{\text{ax}}} = 8.1$ Hz and $J_{4',5'_{\text{ax}}} = 11.1$ Hz, revealing the aminosugar to be 2-deoxy-2-amino-3-methoxy-β-xylopyranose.

Biological activity

Compound **1** showed growth-inhibitory activity against the Gram-positive bacteria *Bacillus subtilis*, *Staphylococcus aureus* and *S. lentus*, but no activity against Gram-negative *Escherichia coli* and the yeast *Saccharomyces cerevisiae*. The MIC of **1** against *B. subtilis* and *S. aureus* was 0.64 μg ml⁻¹ (1 μM).

To determine the cytotoxic activity of **1** against cancer and non-cancer cell lines, two different assays were applied. The crystal violet assay¹⁰ was used to prove the effect of **1** on cell viability, and the lactate dehydrogenase (LDH)-release assay¹¹ indicated the amount of damaged cells due to the destruction of cell membranes. Crystal violet data and LDH-release data showed both growth-inhibitory and cytotoxic activities against all tested cancerous and non-cancerous cell lines (Table 3). EC₅₀ values for a panel of nine cell lines range between 0.17 and 1.62 μM. The growth inhibition is most likely independent from cell density, which is shown for normal human dermal fibroblasts (NHDF) cells in Table 1. The LDH release of the tested cell lines varied dose dependently between 3.68 and 96.83% after 24 h treatment, compared with Triton X-100 (100% positive control). When treated with **1** for only 2 h, the pancreatic cell lines showed no LDH release upon incubation with concentrations of 0.2 and 1.0 μM. Yet, a high LDH release similar to 24 h was observed when 5 μM were used in this short-term assay (data not shown).

DISCUSSION

1 shows a structural relationship to the recently discovered incednine, which was isolated from the culture broth of *Streptomyces* sp. ML694-90F3.¹² Structural differences of **1** and incednine are based in the side chain of the macrolactam ring at C-2, in a different methylation pattern of the sugar (2-deoxy-2-methylamino-β-D-xylopyranose) attached at C-11 and the absence of the sugar (2,3,4,6-tetra-deoxy-4-methylamino-β-D-erythro-hexopyranose) at 4'-OH in **1**.¹² Apart from this, **1** shows the same structural motifs as incednine, also in the

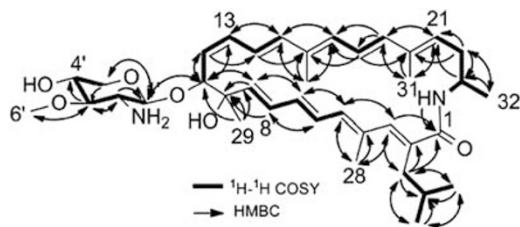


Figure 2 ¹H-¹H-COSY correlations (bold bonds) and selected HMBC correlations (arrows) observed in **1**.

configuration of the double bonds and the all-equatorial arrangement of the substituents of the amino sugar.

As incednine was described showing an interesting interaction with the antiapoptotic oncoprotein Bcl-xL,¹² we investigated the activity of **1** toward different human cell lines. Likewise, it was found that **1** indeed inhibits the growth of various cancer cell lines including pancreatic tumor cell lines, which are difficult to treat with chemotherapeutic agents.¹³ Moreover, **1** inhibited proliferating human skin fibroblasts (NHDF), foreskin fibroblasts (KIF-5) and pancreatic ductal epithelial (HPDE) cell lines. In addition, the LDH release showed dose-dependent cytotoxic effects of **1**. The high LDH release only 2 h after treatment with **1** (5 μM) is likely to be related to an abolishment of the membrane integrity of the target cells. It remains to be shown in what manner normal resting diploid cells respond, and moreover, whether **1** is applicable under *in vivo* conditions in preclinical tumor models without causing severe side effects.

EXPERIMENTAL PROCEDURE

General experimental procedures

UV spectra were obtained on a NanoVue photometer (GE Healthcare, München, Germany). NMR spectra were recorded on a DRX 500 spectrometer (Bruker, Karlsruhe, Germany) at 500 and 125 MHz for ¹H and ¹³C, respectively. The chemical shifts are given in p.p.m. referred to DCM-d₂ as 5.32 p.p.m. (¹H) and 54.00 p.p.m. (¹³C). HPLC-ESI-MS spectra were obtained on a QTRAP 2000 LC-MS/MS spectrometer (Applied Biosystems, Darmstadt, Germany). High-resolution mass spectra were acquired on a benchtop time-of-flight spectrometer (MicroTOF II, Bruker Daltonics, Bremen, Germany) with positive ESI.

The HPLC-DAD system consisted of a HP 1090M liquid chromatograph equipped with a diode-array detector and a HP Kayak XM 600 ChemStation (Agilent Technologies, Waldbronn, Germany). Multiple wavelength monitoring was performed at λ = 210, 230, 260, 280, 310, 360, 435 and 500 nm, and UV-visible spectra were measured from 200 to 600 nm. Sample preparation and chromatographic conditions were performed as described earlier.¹⁴

Producing organism

Strain Tü 6392 was isolated from the rhizosphere of a Norway spruce stand in the Rammert Forest near Tübingen (Germany). A sample taken from the rhizospheric soil was preincubated in HNC medium¹⁵ at 42 °C for 30 min and

Table 3 Growth-inhibitory activity of silvalactam (**1**) against selected cell lines

	EC ₅₀ (μM)		LDH-release assay (% cytotoxicity (s.d.))		
	Mean	95% CI	5 μM	1 μM	0.2 μM
<i>Cancer cell lines</i>					
HT29	0.30	0.27–0.32	58.03 (2.28)	7.28 (9.38)	4.77 (7.58)
KNS62	1.08	0.98–1.19	87.82 (1.61)	29.22 (5.31)	7.42 (1.64)
Colo357	1.62	1.48–1.77	60.69 (1.96)	22.12 (5.46)	–4.22 (2.91)
Panc1	0.60	0.57–0.64	97.72 (1.79)	23.95 (5.39)	–9.75 (4.57)
PancTu1	0.38	0.36–0.39	71.41 (1.46)	52.10 (9.69)	5.68 (9.69)
Panc89	0.31	0.29–0.33	57.92 (4.25)	23.77 (5.28)	13.24 (7.34)
<i>Non-cancer cell lines</i>					
KIF-5	0.50	0.46–0.54	96.83 (2.23)	48.20 (4.38)	0.85 (7.87)
HPDE	0.18	0.17–0.19	58.23 (2.16)	33.27 (6.11)	11.35 (8.96)
NHDF (0.83 × 10 ⁴ cells per cm ²)	0.35	0.34–0.37	92.61 (5.42)	83.45 (3.16)	3.68 (2.22)
NHDF (1.6 × 10 ⁴ cells per cm ²)	0.64	0.62–0.67	—	—	—

Abbreviation: NHDF, Normal human dermal fibroblasts.

Crystal violet and lactate dehydrogenase (LDH)-release data for selected cell lines. EC₅₀ values presented as mean with 95% confidence interval (CI) including 12 different concentrations of **1** with four measurements each. LDH release is shown in three different concentrations (5 μM, 1 μM and 0.2 μM) as mean with s.d.

then transferred to malt extract–yeast extract–glucose agar (ISP-2).¹⁶ Single colonies were picked after 5 days of incubation at 27 °C and transferred to ISP-2 agar plates. Strain Tü 6392 was examined for morphological and chemotaxonomic properties known to be of relevance in streptomycete systematics.^{8,9}

Fermentation and isolation

Batch fermentations of strain Tü 6392 were carried out in a 10-l stirred tank fermentor (New Brunswick Inc., New Brunswick, NJ, USA) in SGG medium that consisted of soluble starch 1%, glucose 1%, glycerol 1%, Bacto peptone 0.5%, cornsteep powder 0.25%, yeast extract 0.2%, NaCl 0.1% and CaCO₃ 0.3% in tap water. The pH was adjusted to 7.3 (5 M HCl) before sterilization. The fermentor was inoculated with 5% by volume of a shake flask culture grown in the same medium at 27 °C in 500 ml Erlenmeyer flasks with a single baffle for 72 h on a rotary shaker at 120 r.p.m. The fermentation was carried out for 7 days at 27 °C with an aeration rate of 0.5 volume air per volume per min and agitation at 250 r.p.m.

For isolation of **1**, the fermentation broth was separated by centrifugation. The culture filtrate (5-l aliquot) was adjusted to pH 8 (5 M NaOH) and extracted three times with EtOAc. The organic extracts were combined and concentrated *in vacuo* to dryness to give a crude product of 280 mg, which was dissolved in CH₂Cl₂ and supplied to a diol-modified silica gel column (45 cm × 1.5 cm; LiChroprep Diol; E. Merck, Darmstadt, Germany). The separation was accomplished by a step gradient from CH₂Cl₂ to 10% MeOH at a flow rate 6 ml min⁻¹. Fractions containing **1** were combined and concentrated *in vacuo* to give a raw product of 64 mg, which was subjected to a preparative reversed-phase HPLC column (Nucleosil-100 C-18, 10 µm, 250 mm × 20 mm; Maisch, Ammerbuch, Germany) with CH₃CN–0.1% HCOOH using linear gradient elution from 35 to 65% CH₃CN within 20 min at a flow rate of 20 ml min⁻¹. The isolation yielded 24 mg of pure **1**.

Antimicrobial assays

The antimicrobial activity spectrum of **1** was determined in concentrations of 0.1–1 mg ml⁻¹ in a microtiter plate assay against *B. subtilis* DSM 10, *S. aureus* DSM 20231, *E. coli* K12, *S. cerevisiae* ATCC 9080 and *Botrytis cinerea* Tü 157.

The minimal inhibition concentration of **1** was tested in a microtiter plate assay using *B. subtilis* DSM 10 and *S. aureus* DSM 20231. Overnight cultures of the test organisms in Bacto nutrient broth were diluted to an OD ($\lambda = 578$ nm) of 0.025. The assay was prepared by transferring 5 µl of standard concentrations (0.4 µM–4 mM) of **1** dissolved in DMSO into one well of a 96-well microtiter plate containing 195 µl of cell suspension culture. After incubation for 24 h at 37 °C and 100 r.p.m., the bacterial growth was examined visually.

Viability and cytotoxicity assays

Foreskin fibroblasts KIF5, colon carcinoma cell line HT29,¹⁷ pancreatic carcinoma cell lines Panc1, PancTu1, Panc89 and Colo357,¹⁸ and lung carcinoma cell line KNS62¹⁹ were maintained in RPMI 1640 medium (Gibco, Berlin, Germany). The medium was supplemented with 10% fetal calf serum, 5% glutamax (PAA Laboratories GmbH, Pasching, Austria) and 5% sodium pyruvate (PAA Laboratories GmbH) in cell culture flasks. HPDE cells were cultivated in HPDE medium (Gibco), containing 50% RPMI 1640 with 10% fetal calf serum and 5% glutamax and 50% keratinocyte medium with 2.5 µg epidermal growth factor and 25 mg pituitary extract (Invitrogen, Darmstadt, Germany). NHDF (Promocell, Heidelberg, Germany) were cultivated in a mixture of 50% full Fibroblast Growth Medium (Promocell) mixed with RPMI 1640 medium, which was supplemented with 10% fetal calf serum, 5% glutamax and 5% sodium pyruvate. All cells were incubated at 37 °C in a 5% CO₂ humidified environment.

For crystal violet assays, cells were detached with accutase (PAA Laboratories GmbH) and seeded in 96-well plates in a concentration of 1.6 × 10⁴ cells per cm². After 24 h, a serial dilution of **1** (12 dilution steps ranging from 5–0.05 µM), which were prepared in DMSO (at most 0.5% DMSO in cell culture medium), was added to each 100-µl cell culture medium. About 0.5% DMSO was used as control. The medium was removed after 72 h and cells were stained with 50 µl of crystal violet (E. Merck; 0.5% crystal violet in 20%

MeOH) for 20 min. The wells were air-dried overnight after repeated washing with H₂O. The crystalline dye was dissolved in 100% MeOH for 30 min, and OD was measured in a microplate reader (Tecan, Crailsheim, Germany) at $\lambda = 590$ nm and a reference wavelength of 700 nm.

For LDH-release assays, the cells were seeded as described for the crystal violet assay and incubated with 200 µl of different concentrations of **1** (5 µM, 1 µM and 0.2 µM), or 1% Triton X-100 (100% control) or 0.5% DMSO (zero control). After incubation for 24 h, the test (LDH Cytotoxicity Detection Kit; Clontech, Heidelberg, Germany) was performed using 100 µl of cell culture supernatant according to the manual. Absorbance at $\lambda = 492$ nm ($\lambda = 650$ nm as reference) was measured using a microplate reader (Tecan).

EC₅₀ values of crystal violet data were calculated with Prism 4 (GraphPad Software, Inc., La Jolla, CA, USA) using a nonlinear regression model. Cytotoxicity was calculated with Excel 2010 (Microsoft, Redmond, WA, USA). Each dilution step was tested in four wells; crystal violet experiments were repeated twice.

ACKNOWLEDGEMENTS

Financial support from the Deutsche Forschungsgemeinschaft (Graduate College 685 'Infection Biology'; DS), the Cluster of Excellence 'Unifying Concepts in Catalysis' coordinated by the Technische Universität Berlin is gratefully acknowledged. We thank Andreas Kulik, Universität Tübingen, for assistance in fermentations, and Dr Heidi Zinecker, KiWiZ, IFM-GEOMAR, Kiel, for bioactivity assays.

- Helaly, S.E. *et al.* Langkolide, a 32-membered macrolactone antibiotic produced by *Streptomyces* sp. Acta 3062. *J. Nat. Prod.* (2012) (in press).
- Watve, M. G., Tickoo, R., Jog, M. M. & Bhole, B. D. How many antibiotics are produced by the genus *Streptomyces*? *Arch. Microbiol.* **176**, 386–390 (2001).
- Clardy, J., Fischbach, M. A. & Walsh, C. T. New antibiotics from bacterial natural products. *Nat. Biotechnol.* **24**, 1541–1550 (2006).
- Goodfellow, M. & Fiedler, H.-P. A guide to successful bioprospecting: informed by actinobacterial systematics. *Antonie van Leeuwenhoek* **98**, 119–142 (2010).
- Fiedler, H.-P. Biosynthetic capacities of actinomycetes. 1. Screening for novel secondary metabolites by HPLC and UV-visible absorbance libraries. *Nat. Prod. Lett.* **2**, 119–128 (1993).
- Mitchell, S. S., Nicholson, B., Teisan, S., Lam, K. S. & Potts, B. C. Aureoverticillactam, a novel 22-atom macrocyclic lactams from the marine actinomycete *Streptomyces aureoverticillatus*. *J. Nat. Prod.* **67**, 1400–1402 (2004).
- Schulz, D. *et al.* Piceamycin and its *N*-acetylcysteine adduct is produced by *Streptomyces* sp. GB 4-2. *J. Antibiot.* **62**, 513–518 (2009).
- Williams, S. T., Goodfellow, M. & Alderson, G. in *Bergey's Manual of Systematic Bacteriology*. Vol. 4 (eds Williams *et al.*) 2452–2492 (Williams & Wilkins, Baltimore, USA, 1989).
- Manfio, G. P., Zakrzewska-Czerwinska, J., Atalan, E. & Goodfellow, M. Towards minimal standards for the description of *Streptomyces* species. *Biotechnologia* **8**, 228–237 (1995).
- Trauzold, A. *et al.* TRAIL promotes metastasis of human pancreatic ductal adenocarcinoma. *Oncogene* **25**, 7434–7439 (2006).
- Kater, B. *et al.* Iron containing anti-tumoral agents: unexpected apoptosis-inducing activity of a ferrocene amino acid derivative. *J. Cancer Res. Clin. Oncol.* **137**, 639–649 (2001).
- Futamura, Y. *et al.* Discovery of incednine as a potent modulator of the anti-apoptotic function of Bcl-xL from microbial origin. *J. Am. Chem. Soc.* **130**, 1822–1823 (2008).
- Sebens, S. & Kalthoff, H. Emerging therapeutic agents for pancreatic cancer therapy—where are we and where we have to go? *Anticancer Agents Med. Chem.* **11**, 408–410 (2011).
- Nachtigall, J. *et al.* Benzoxacystol, a benzoxazine-type enzyme inhibitor from the deep-sea strain *Streptomyces* sp. NTK 935. *J. Antibiot.* **64**, 453–457 (2011).
- Nonomura, H. & Hayakawa, M. in *Biology of Actinomycetes '88* (eds Okami, Y. *et al.*) 288–293 (Japan Scientific Societies Press, Tokyo, Japan, 1988).
- Shirling, E. B. & Gottlieb, D. Methods for characterization of *Streptomyces* species. *Int. J. Syst. Bacteriol.* **16**, 313–340 (1966).
- Vogel, I. *et al.* A human carcinoma model in athymic rats reflecting solid and disseminated colorectal metastases. *Langenbecks Arch. Surg.* **383**, 466–473 (1998).
- Sipos, B. *et al.* A comprehensive characterization of pancreatic ductal carcinoma cell lines: towards the establishment of an *in vitro* research platform. *Virchows Arch.* **442**, 444–452 (2003).
- Schniewind, B. *et al.* Combination phenylbutyrate/gemcitabine therapy effectively inhibits *in vitro* and *in vivo* growth of NSCLC by intrinsic apoptotic pathways. *J. Carcinog.* **23**, 5–25 (2006).